J Mater Sci (2010) 45:2688–2695
DOI 10.1007/s10853-010-4250-9

Experimental and numerical study of the elastic properties of PMI foams

Jie Wang · Hai Wang · Xiuhua Chen · Yin Yu

Received: 14 October 2009 / Accepted: 19 January 2010 / Published online: 2 February 2010

Abstract The elastic properties of polymethacrylimide (PMI) foams were investigated experimentally and numerically. Standard tests were carried to measure the mechanical properties of ROHACELL® WF and RIST grades foams. The tetrakaidekahedral unit cell was adopted to generate a 3D representative volume element (RVE) for the microstructure of PMI foams. It is assumed that the RVE represents the foam within the framework of elasticity. The RVE models thus created were analyzed with periodic boundary conditions to obtain the elastic properties of PMI foams by using finite element analysis (FEA). The numerical results were compared with the experimental data and the prediction of existing theoretical models, and the proposed model was found to give the best prediction for the effective modulus of PMI foams. Parameter studies were also carried out using the RVE models to investigate the effect of the foam cell size and cell thickness on the effective modulus of PMI foams.

Introduction

Foam materials have been widely used in a variety of applications including aircrafts, satellite launch vehicles, wind power plant, aerospace and ship building, as well as construction and the manufacture of sports equipment [1].This is due to their excellent properties such as low density, high heat distortion temperature, outstanding strength-to-weight ratio, ease of machining, excellent fatigue behavior, and good dielectric properties. Polymethacrylimide (PMI) rigid foam such as ROHACELL® (Evonik Röhm GmbH, Germany) has thermal stability up to 455 °F/235 °C, low smoke density, and no release of corrosive emissions upon combustion, which can meet some extreme demands both in respect to workability and in operation.

The increasing engineering applications of foam materials made it necessary to understand their mechanical properties, and a significant amount of work has been done by different researchers.

In particular, Gibson and Ashby have done extensive work by micro-mechanics to study the mechanical behavior of cellular solids in [2]. Mills, Zhu et al. [3, 4] also made great effort to investigate the deformation mechanism in open-cell foams.

Various micromechanics models for two- or three-dimensional open/closed-cell foams have been developed to investigate the relations between mechanical properties and structural characteristics of the foam cells, and they were summarized in [5]. Of which, the tetrakaidecahedral foam model [6], which consists of 14-sided polyhedra in a body centered cubic (BBC) arrangement was preferred by many researchers [7–10], and periodic conditions were also considered [11].

Finite element method (FEM) has been an important approach to predict the mechanical properties of foam materials [12, 13]. In most cases, different microstructures (regular and irregular) have been employed to study the influence of structural irregularities and geometry

J. Wang
School of Naval Architecture, Ocean and Civil Engineering, Shanghai Jiao Tong University, No.800 Dongchuan Rd., Shanghai 200240, People's Republic of China
e-mail: vincent0306@gmail.com

H. Wang (✉) · X. Chen · Y. Yu
School of Aeronautics and Astronautics, Shanghai Jiao Tong University, No.800 Dongchuan Rd., Shanghai 200240, People's Republic of China
e-mail: wanghai601@sjtu.edu.cn

properties on the mechanical behavior of foam materials [14–16]. In particular, Voronoi tessellation which can model the formation of foams from coagulation of gas bubbles in liquid was used to account for the random geometry of the foam [17–21].

As for PMI foams, Lakes et al.[5] used the Ashby's theory of the micro-mechanics of cellular materials to study the mechanical properties of PMI foams based on the tetrakaidecahedral unit cell shape; Lakes et al.[22] also examined the size effects due to Cosserat elasticity and surface damage of PMI foams, according to their study, ROHACELL® PMI foam behaves as a Cosserat elastic material and the Cosserat elastic constants are determined by the method of size effects, but as the solutions for the Cosserat solids depend on the elastic constants in complex ways, it makes it difficult to numerically analyze a foam material based on the constitutive equations. A. Roth (in 8th International Conference on Sandwich Structures, FEUP, Porto, 2008) discussed the failure criteria and fracture toughness for ROHACELL® PMI foams based on experiments and numerical analysis, which facilitated the applications of these foams.

Like most of the closed-cell foams, the mechanical properties of PMI foam materials depend on the material from which they are made, their relative densities, and their internal geometrical structures. In this article, elastic properties of PMI foams were investigated by standard tests and linear FE analysis of RVE models. Parameter studies were also carried out using the FE models to investigate the effect of the foam cell size and thickness on the effective modulus of PMI foams.

PMI foam of ROHACELL®

ROHACELL® is a family of PolyMethacrylImide (PMI) foams, and it is the only homogeneous and 100% closed-cell foam. ROHACELL® foams are produced by thermal expansion of a copolymer sheet of methacrylic acid and methacrylonitrile. During the foaming process, the copolymer sheet is converted to polymethacrylimid (PMI). Alcohol is used as a blowing agent; thus ROHACELL® contains no fluorinated carbon hydrates and is halogen-free (DEGUSSA, Röhm GmbH (2004) Data CD "ROHACELL®—The Core for Sandwich Solutions"). As a result of the process, rigid closed-cell foam with a very homogeneous cell structure is obtained (Fig. 1).

The cell walls of ROHACELL® foams are of almost uniform thickness. Figure 2 shows the detailed morphology of ROHACELL® foams; it can be seen that the cells of ROHACELL® foams are almost the same size. When it is foamed there are no neck formations with material concentration at the webs or corners as a low viscosity material such as PUR. It can be seen from Fig. 2 that the edges have

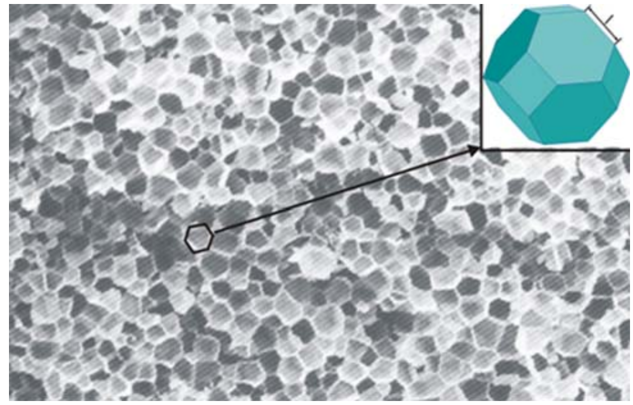

Fig. 1 REM of ROHACELL® foam and the unit cell of FEM models

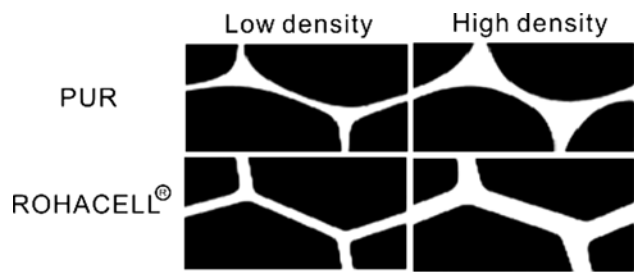

Fig. 2 Morphology comparison of ROHACELL® and PUR foams

no Plateau border section [23]. So, when imperfections and irregularities are not considered, two parameters would be enough to depict the geometry of the PMI foam cells, which are the cell-wall thickness and the cell edge length. The tetrakaidecahedron (Thompson, 1887) which is the only polyhedron that packs with identical units to fill space, which has a relatively low anisotropy, and which nearly satisfies the minimum surface energy conditions, is really a good geometry model for PMI foam cell.

Mechanical tests and property characterization

The closed-cell PMI foams considered in this article are ROHACELL® WF and RIST grades foams from Evonik Röhm GmbH. The experimental characterization of the ROHACELL® foams has been performed by Evonik using tensile, compressive, and shear tests. The tensile test has been carried out following the DIN 53455/ISO 527-2/ASTM D 638 standard. The compressive test has been carried out following the DIN 53421 standard. The shear test has been carried out following the DIN 53294/ASTM C 273 standard. The mechanical properties of the ROHACELL® WF and RIST grades foams are listed in Table 1. (Most of the ROHACELL® foams have a Poisson's ratio between 0.37 and 0.38 at room temperature. Here we take 0.375 as a reference value.)

Table 1 Mechanical properties of ROHACELL® foams

ROHACELL® foam grade	WF 51	WF 71	WF 110	RIST 51	RIST 71	RIST 110
Foam Density, $\rho[kg/m^3]$	54.1	75.6	111.4	52.1	77.6	110.7
Young's modulus, $E[MPA]$	77.4	114.5	181.9	70.4	123.4	192.3
Shear modulus, $G[MPA]$	32.0	46.3	69.2	30.0	45.4	72.2
Poisson's ratio, ϑ	0.375	0.375	0.375	0.375	0.375	0.375

Table 2 Density, average cell-wall thickness, and average cell size of ROHACELL® foams

ROHACELL® foam grade	WF 51	WF 71	WF 110	RIST 51	RIST 71	RIST 110
Average cell size, $a[\mu m]$	714	743	562	296	295	219
Average cell wall thickness, $t[\mu m]$	9.5	10	12.5	4	5.5	7.25

The solid foam material was assumed to be isotropic rigid polyurethane with the Young's modulus $E_s = 1.6$ GPa, Poisson's ratio $v* = 0.3$, and density $\rho^* = 1200$ kg/m^3.The microstructure dimensions were determined for ROHACELL® foams by Evonik and summarized in Table 2.

Effective modulus theory

Foams and regular lattice structures have been extensively studied in the past to improve the understanding of their mechanical properties. Using dimensional analysis, equations for Young's modulus, shear modulus, and Poisson's ratio of closed-cell foam were given by Gibson and Ashby [2] in terms of relative density. In their work, there are three mechanisms that contribute to the linear-elastic response of closed-cell foams: (i) cell-wall bending; (ii) edge contraction and membrane stretching; (iii) enclosed gas pressure.

These equations can be expressed as follows:

$$\frac{E^*}{E_s} = \phi^2\left(\frac{\rho^*}{\rho_s}\right)^2 + (1-\phi)\frac{\rho^*}{\rho_s} + \frac{p_0(1-2v*)}{1-\rho^*/\rho_s} \quad (1)$$

$$\frac{G^*}{E_s} \approx \frac{3}{8}\left[\phi^2\left(\frac{\rho^*}{\rho_s}\right)^2 + (1-\phi)\frac{\rho^*}{\rho_s}\right] \quad (2)$$

$$v = \frac{1}{3} \quad (3)$$

Besides, Chen and Lakes [5] also developed a micromechanical model for ROHACELL® closed-cell foams based on the tetrakaidecahedral unit cell, which predicts

$$\frac{E^*}{E_s} = \frac{0.343 + 0.832\frac{\rho^*}{\rho_s}\rho^*}{0.684 + \frac{\rho^*}{\rho_s}\quad \rho_s} \text{ with } \frac{\rho^*}{\rho_s} = 1.18\frac{t}{l} \quad (4)$$

For these equations, ρ^* is the density of the foam, ρ_s is the density of the solid form of the material, ρ^*/ρ_s is the relative density. ϕ is the fraction of the foamed material in the cell edges of the individual cell (with the remainder in the walls), p_0 is the initial pressure in the foam cells (usually atmospheric pressure). l and t are the characteristic cell edge length and cell thickness, respectively.

Finite element analysis

Geometry and RVE model

The commercial software MSC.NASTRAN was used for the linear analysis, with MSC.Patran as a processor. The tetrakaidekahedral model (Fig. 1) with flat faces is adopted as the unit cell. An orthogonal coordinate was set with the origin at the center of the unit cell and the three orthogonal axes normal to the square face of the unit cell. The RVE of the foam structure was formed by periodic repetition of unit cell within three orthogonal directions, and the cell number in each orthogonal direction was defined as the model size, n. The sections of cell walls between the outer unit cells and around the corner of the RVE were also modeled to reflect the real structure of foams and form a cubic model. An RVE of size 4 is shown in Fig. 3.

All cell walls in the model were assumed to be made of the same material and have the same thickness as the measured values in Table 2, except that cell walls which coincide with the model's periodic boundaries (which will be discussed below) were given half the thickness. The

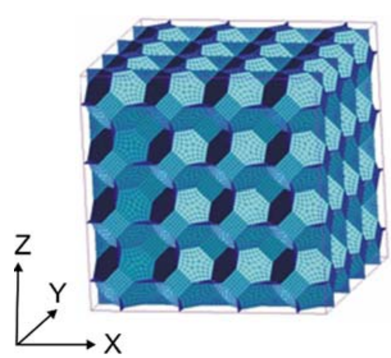

Fig. 3 RVE with 91 cells (size 4) and the elements

relationship between the cell size a and cell edge length l was taken to be: $l = a$. Quadrilateral linear shell elements (QUAD4) from the MSC.NASTRAN element library were used to model the cell walls. Patran Command Language (PCL) tools were used to develop a series of RVE models with different model size and to realize the periodic boundary conditions.

Boundary conditions

Periodic boundary conditions as stated by Suquet (1987) are imposed on the six sides of the models. The periodic conditions on the boundary ∂V is

$$u_i = \overline{\varepsilon_{ik}} + u_i^* \quad \left(u_i^* \text{ is periodic}\right) \tag{5}$$

As the models were formed by periodic repetition of unit cell within three orthogonal directions, the mesh grids in the opposite sides of the rectangular RVE are the same, which satisfies the requirement of the periodic boundary conditions.

The six sides of the model were defined as follows: side 1: $x = 0$; side 2: $x = h$; side 3: $y = 0$; side 4: $y = h$; side 5: $z = 0$; side 6: $z = h$, where h is the height of the model: $h = n \times a$.

For different loading cases, as in [24], the periodic boundary conditions can be interpreted as: uniaxial compression/tension (along z direction) case:

$$\begin{aligned}
&u_i^1 - u_i^2 = 0 \ (i = 1,2,3,4,5,6)\\
&u_i^3 - u_i^4 = 0 \ (i = 1,2,3,4,5,6)\\
&u_3^5 - u_3^6 = \delta_1, u_i^5 - u_i^6 = 0 \ (i = 1,2,4,5,6)\\
&u_i^A = 0 \ (i = 1,2,3) \ \text{(to eliminate the rigid body motion)}
\end{aligned} \tag{6}$$

pure shear (in x–z plane) case:

$$\begin{aligned}
&u_3^1 - u_3^2 = \delta_2, u_i^1 - u_i^2 = 0 \ (i = 1,2,4,5,6)\\
&u_i^3 - u_i^4 = 0 \ (i = 1,2,3,4,5,6)\\
&u_1^5 - u_1^6 = \delta_2, u_i^5 - u_i^6 = 0 \ (i = 2,3,4,5,6)\\
&u_i^A = 0 \ (i = 1,2,3) \ \text{(to eliminate the rigid body motion)}
\end{aligned} \tag{7}$$

where the superscript numbers refer to the different sides, and the subscript numbers refer to the six freedom of displacement of the grid, point A is a center point of the RVE model. The constant δ_1 represents the average stretch or contraction of the RVE model due to the action of the normal traction components, whereas δ_2 corresponds to the shear deformation due to the shear traction components.

Calculation of effective properties

As the least modulus of the foams here is 30 MPa and the atmospheric air pressure is 0.1 MPa, the internal air pressure contribution to the stiffness of the PMI foams was neglected.

As stated earlier, the PMI foams are thought to be isotropic. It is assumed that the average mechanical properties of the RVE are equal to the average properties of the particular PMI foams. Then the homogenization method based on micro-mechanical is used to calculate the elastic properties of PMI foams. The average stresses and strains in a RVE are defined by:

$$\bar{\varepsilon}_{ij} = \frac{1}{V}\int_V \varepsilon_{ij}\mathrm{d}V \quad (i,j = 1,2,3) \tag{8}$$

$$\bar{\sigma}_{ij} = \frac{1}{V}\int_V \sigma_{ij}\mathrm{d}V \quad (i,j = 1,2,3) \tag{9}$$

where V is the total volume of the elements in the RVE; ε_{ij} and σ_{ij} are the actual local stress and strain tensor components in the RVE.

The $\bar{\sigma}_{ij}$ and $\bar{\varepsilon}_{ij}$ for independent loading cases as defined above can be obtained by conducting linear analysis of the RVE model. Then, the effective elastic constants of PMI foams can be calculated according to the following equation:

$$\bar{\sigma}_{ij} = \overline{C}_{ijkl}\bar{\varepsilon}_{kl} \ (i,j,k,l = 1,2,3) \tag{10}$$

Comparison of the results

For a fixed mesh size, model size sensitivity analyses were performed for all the models. The Poisson's ratio and Relative shear modulus of the foams were analyzed using FE models with a bigger and bigger model size. A suitable model size was established once a plateau in the calculated values of Poisson's ratio and Relative shear modulus was found. It can be seen from the Fig. 4 that, under the periodic boundary condition, an RVE of small model size would be adequate to model the elastic properties of PMI foams.

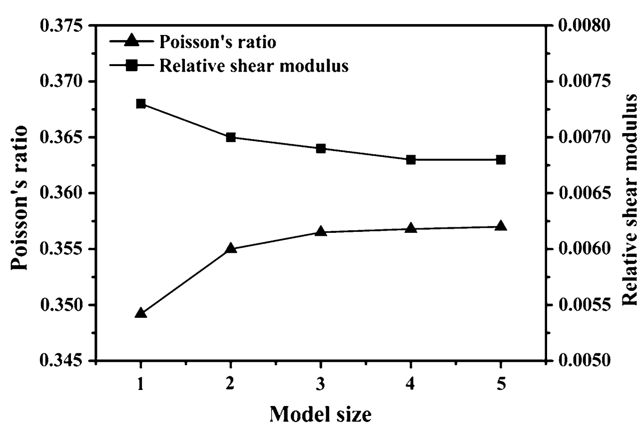

Fig. 4 Effects of model size on the relative shear modulus and Poisson's ratio of WF51 foam

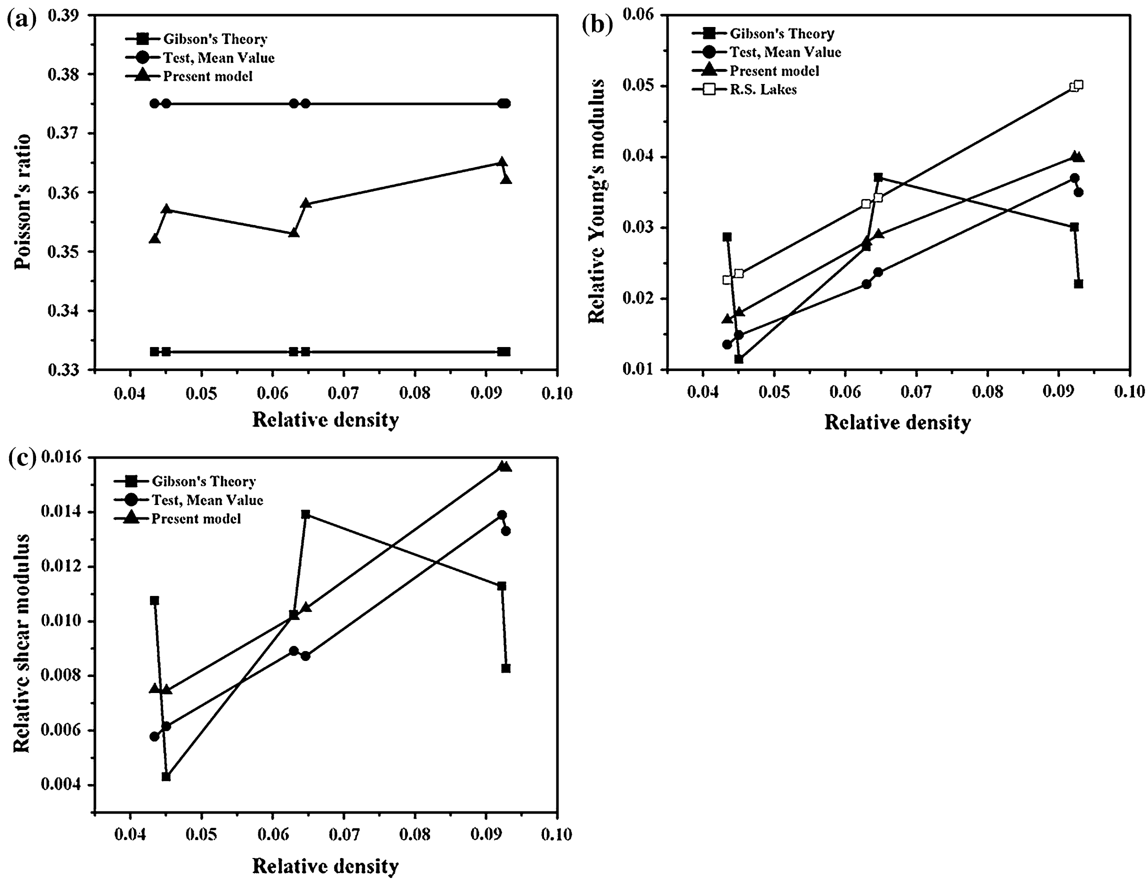

Fig. 5 Comparison of the results: **a** Poisson's ratio of PMI foams, **b** relative Young's modulus of PMI foams, **c** relative shear modulus of PMI foams

A comparison between the experimentally measured Poisson's ratio (ν), Young's modulus (E), and shear modulus (G) of ROHACELL® WF and RIST grades foams and predicted by the present model and the corresponding theoretical predictions were shown in Fig. 5. The FEA and experimental results were for WF70, 110 and 200, RIST70, 110 and 200 foams. The theoretical predictions of the foams were calculated using Gibson's and Chen and Lakes's semi-empirical Eqs. 1–4.

For the Gibson's equations, ϕ was calculated by Eq. 11, which is based on the tetrakaidecahedral unit cell shape for closed-cell foams [25].

$$\phi = \frac{12A_e}{11.31l^2}\left(\frac{1}{\rho^*/\rho_s}\right) \tag{11}$$

where, A_e is the area contained in an edge cross-section and can be expressed in terms of the face thickness, t, as

$$A_e = \frac{t^2}{2}\left(\frac{1}{1.932} + \sqrt{\frac{3}{2}}\right) \tag{12}$$

The Poisson's ratios of PMI foams predicted by the present model are compared with test data and Gibson's theory in Fig. 5a. It could be seen that neither the prediction from the present model nor the Gibson's theory predicts the right Poisson's ratio for PMI foams. Possible reasons are: first, it is hard to measure the Poisson's ratio of foam material, the constant value of 0.375 is only a reference value as stated earlier; second, the elastic behavior of PMI foam does not conform to that of isotropic material exactly. However, the predictions from the present model, which varied between 0.35 and 0.365, are more nearer to the tested data than the Gibson's constant value of 1/3.

Figure 5b and c compare, respectively, the relative Young's modulus (E^*/E_s) and relative shear modulus (G^*/E_s) predicted by the present model with the test data and those from Gibson's and Lakes's theories. It can be seen that both the present model and Lakes's theory overestimate the two moduli of PMI foams, but general trends are in agreement with the test data, with the present model providing much more reasonable estimates. The Gibson's theory does not give the right predictions for both the relative Young's modulus and the relative shear modulus.

Parameter study

Parameter studies were performed to investigate the effect of foam cell geometry on the elastic properties of PMI foams. The studies were confined to linear analysis of the RVE models with cell size varied between 200 and 800 μm and cell thickness varied between 4 and 13 μm.

Figure 6a and b contain plots of the calculated relative Young's modulus and relative shear modulus as a function of the cell size, *n*, while the cell thickness holds constants as 4, 8, and 12 μm, which stand for thin, middle thick, and thick cell foams, respectively. It is noted that the cell size has different effects on Young's and shear modulus. For thin cell foams, the two moduli initially decrease rapidly as the cell size increases and then increase gradually when the cell size exceeds 590 μm. For middle thick cell foams, the Young's modulus decreases linearly as the cell size increases, the shear modulus decreases rapidly as the cell size increases and then increases softly when the cell size exceeds 720 μm. For thick cell foams, the Young's modulus increases linearly as the cell size increases, the shear modulus decreases gradually as the cell size increases and then increases rapidly when the cell size exceeds 460 μm. Also noted that, the curve of the shear modulus for the thicker cell foams lies above the one for the thinner.

Figure 6c and d contain similar plots of the calculated relative Young's modulus and relative shear modulus as a function of the cell thickness, *t*, while the cell thickness hold constants as 200,500, and 700 μm, which stand for small, middle large, and large cell foams, respectively. For the small cell foams, the Young's modulus increases significantly with an increase in cell thickness and then decreases rapidly when the cell thickness exceeds 8 μm, the shear modulus increases gradually as the cell thickness increases and then decreases softly when the cell thickness exceeds 11 μm. For middle large cell foams, the Young's modulus increases softly as the cell thickness increases and then decreases gradually when the cell thickness exceeds 11 μm, the shear modulus increases linearly as the cell thickness increases. For large cell foams, both of the two moduli decrease as the cell thickness increases and then increase when the cell thickness exceeds 5 and 6 μm, respectively, with the shear modulus changes more rapidly.

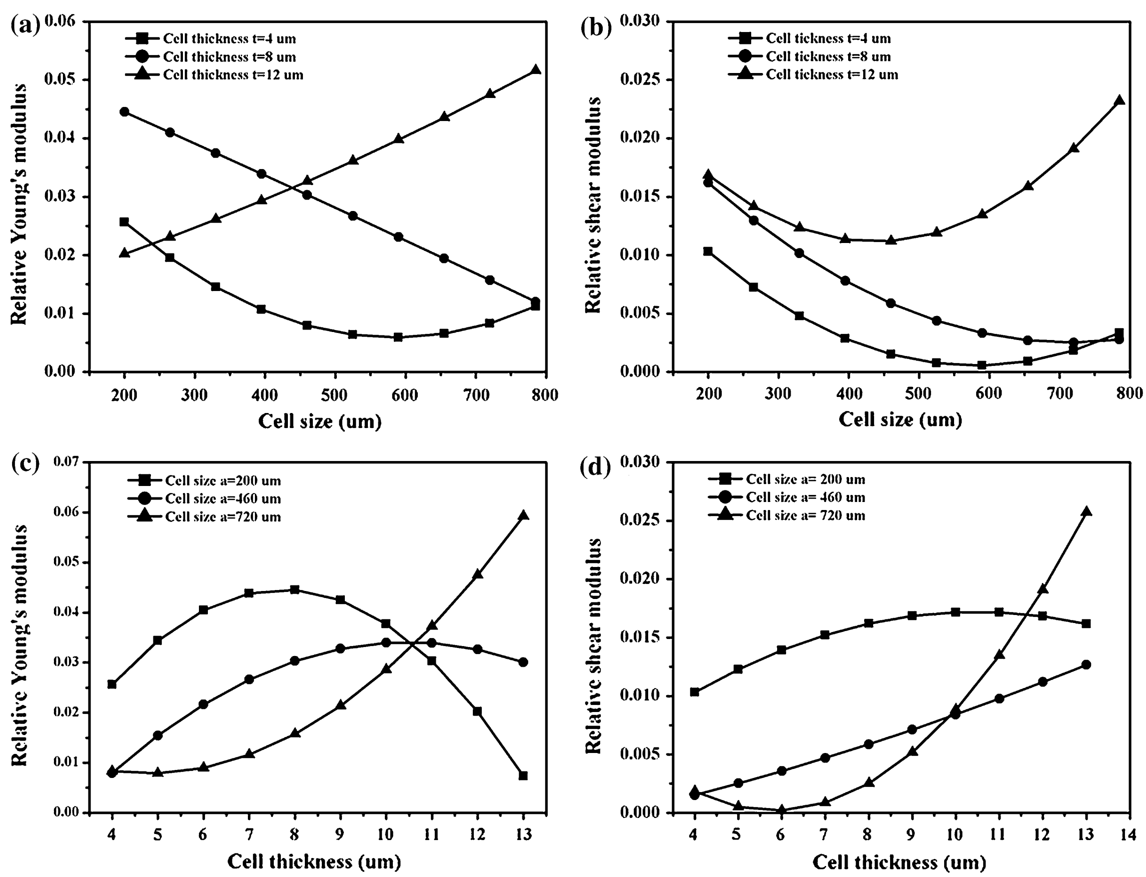

Fig. 6 The effect of foam cell geometry on the elastic properties of PMI foams: **a** the effect of varying the cell size on relative Young's modulus, **b** the effect of varying the cell size on relative shear modulus, **c** the effect of varying the cell thickness on relative Young's modulus, **d** the effect of varying the cell thickness on relative shear modulus

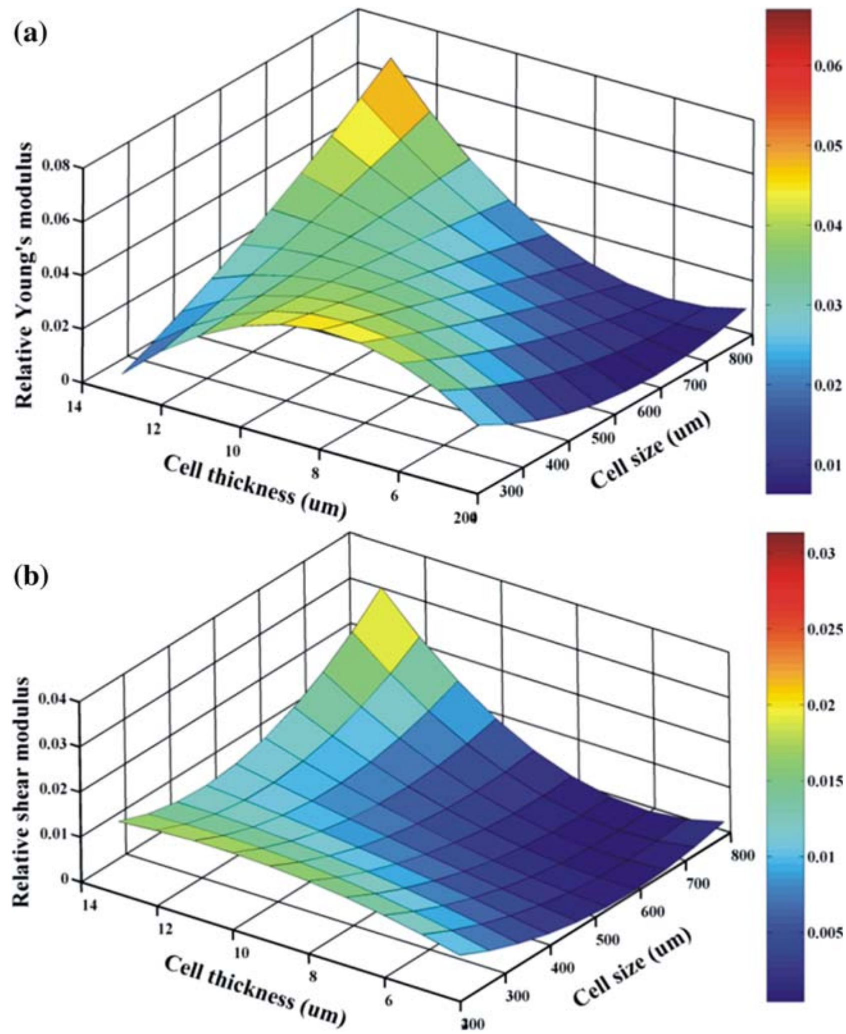

Fig. 7 Response surfaces: **a** response of relative Young's modulus, **b** response of relative shear modulus

In order to find the overall effect of cell size and cell thickness on the elastic properties of PMI foams, the cell size was varied over 10 different values and the cell thickness by 10 different values, simultaneously. Figure 7 plots the response surfaces of the relative Young's and shear modulus with respect to the two geometry parameters.

It can be seen that the two moduli have the same general trend with the two geometry parameters varied and both of the response surfaces have two peaks. As expected, the two first peaks appear simultaneously when the cell size and cell thickness reach the maximum values, 200 and 13 μm, respectively. The second peak of the Young's modulus appears at the point with cell size of 200 μm and cell thickness of 9 μm, while the second peak of the shear modulus appears when the cell size is 200 μm and the cell thickness is 12 μm. It can also be seen that the response surface is the most sensitive when the cell size and the cell thickness are large.

Conclusions

- On the basis of the experimental tensile, compressive and shear tests performed the mechanical characteristics of ROHACELL WF and RIST grades PMI foams were obtained, together with different theoretical predictions and measured foam density, these results show that the elastic properties of PMI foams cannot be properly predicted just by relative density as stated by Gibson's semiempirical equations.
- Finite element RVE models bases on tetrakaidekahedral unit cell were proposed and analyzed with periodic boundary conditions to predict the elastic properties of PMI foams. The FEM predictions were compared with the test data and theoretical values; it was found that the RVE models gave the best predictions for PMI foams, which validated the further use of these models.
- Parameter studies were carried out using the RVE models to investigate the effect of foam cell geometry

on the effective modulus of PMI foams. According to the parameter studies, the foam cell size and cell thickness can greatly influence the elastic properties of PMI foams: thin and middle thick cell foams with large cell size tend to have smaller Young's and shear modulus, while the thick cell foams with large cell size tend to have larger Young's and shear modulus. The effect is especially large when the cell size and cell thickness are large.
- The proposed model is suitable to perform engineering designs for PMI foams. The desired elastic properties of PMI foams can be reached by choosing the proper foam cell size and cell thickness, which might be used to tailor new foams by demand that are not often experimentally available.

Acknowledgements The authors wish to thank Mr.Hu Pei of Evonik Corporation for providing the necessary data of ROHACELL® PMI foams, and his useful suggestions are also gratefully acknowledged.

References

1. Zenket D (1997) The handbook of sandwich construction, 2nd edn. EMAS Press, London
2. Gibson LJ, Ashby MF (1997) Cellular solids: structure and properties, 2nd edn. Cambridge University Press, Cambridge
3. Mills NJ, Zhu HX (1999) J Mech Phys Solids 47:669
4. Zhu HX, KnottT JF, Mills NJ (1997) J Mech Phys Solids 45:319
5. Chen CP, Lakes RS (1995) Cell Polym 14:186
6. Kelvin Lord (1887) Phil Mag 24:503
7. Li K, Gao XL, Roy AK (2003) Compos Sci Technol 63:1769
8. Warren WE, Kraynik AM (1997) J Appl Mech 64:787
9. Gong L, Kyriakides S, Triantafyllidis N (2005) J Mech Phys Solids 53:771
10. Gong L, Kyriakides S, Jang WY (2005) Int J Solids Struct 42:1355
11. Laroussi M, Sab K, Alaoui A (2002) Int J Solids Struct 39:3599
12. Luxner MH, Stampfl J, Pettermann HE (2005) J Mater Sci 40:5859. doi:10.1007/s10853-005-5020-y
13. Luxner MH, Woesz A, Stampfl J, Fratzl P, Pettermann HE (2009) Acta Biomater 5:381
14. Luxner MH, Stampfl J, Pettermann HE (2007) Int J Solids Struct 44:2990
15. Grenestedt JL (2005) J Mater Sci 40:5853. doi:10.1007/s10853-005-5019-4
16. Grenestedt JL, Bassinet Franck (2000) Int J Mech Sci 42:1327
17. Van Der Burg MWD, Shulmeister V, Van Der Geissen E, Marissen R (1997) J Cell Plast 33:31
18. Zhu HX, Hobdell JR (2000) Acta Mater 48:4893
19. Shulmeister V, Van Der Burg MWD, Van Der Giessen E, Marissen R (1998) Mech Mater 30:125
20. Roberts A (2001) Acta Mater 49:189
21. Robertsa AP, Garboczia EJ (2002) J Mech Phys Solids 50:33
22. Anderson WB, Lakes RS (1994) J Mater Sci 29:6413. doi:10.1007/BF00353997
23. Kraynik AM, Warren WE (1994) In: Hilyard NC, Cunningham A (eds) Low density cellular plastics. Chapman and Hall, London
24. Xia Zihui, Zhang Yunfa, Fern Ellyin (2003) Int J Solids Struct 40:1907
25. Simone AE, Gibson LJ (1998) Acta Mater 46:2139